ORIGINAL RESEARCH

Carbonic Anhydrase Inhibition Ameliorates Inflammation and Experimental Pulmonary Hypertension

Hannes Hudalla[1,2,3*], Zoe Michael[1,3*], Nicolas Christodoulou[1], Gareth R. Willis[3,4], Angeles Fernandez-Gonzalez[3,4], Evgenia J. Filatava[1], Paul Dieffenbach[3,5], Laura E. Fredenburgh[3,5], Robert S. Stearman[6], Mark W. Geraci[6], Stella Kourembanas[1,3,4‡], and Helen Christou[1,3,4]

[1]Department of Pediatric Newborn Medicine and [5]Division of Pulmonary and Critical Care Medicine, Brigham and Women's Hospital, Boston, Massachusetts; [2]Department of Neonatology, Heidelberg University Children's Hospital, Heidelberg, Germany; [3]Harvard Medical School, Boston, Massachusetts; [4]Division of Newborn Medicine, Boston Children's Hospital, Boston, Massachusetts; and [6]Division of Pulmonary, Critical Care Medicine, Sleep, and Occupational Medicine, Department of Medicine, School of Medicine, Indiana University, Indianapolis, Indiana

Abstract

Inflammation and vascular smooth muscle cell (VSMC) phenotypic switching are causally linked to pulmonary arterial hypertension (PAH) pathogenesis. Carbonic anhydrase inhibition induces mild metabolic acidosis and exerts protective effects in hypoxic pulmonary hypertension. Carbonic anhydrases and metabolic acidosis are further known to modulate immune cell activation. To evaluate if carbonic anhydrase inhibition modulates macrophage activation, inflammation, and VSMC phenotypic switching in severe experimental pulmonary hypertension, pulmonary hypertension was assessed in Sugen 5416/hypoxia (SU/Hx) rats after treatment with acetazolamide or ammonium chloride (NH_4Cl). We evaluated pulmonary and systemic inflammation and characterized the effect of carbonic anhydrase inhibition and metabolic acidosis in alveolar macrophages and bone marrow–derived macrophages (BMDMs). We further evaluated the treatment effects on VSMC phenotypic switching in pulmonary arteries and pulmonary artery smooth muscle cells (PASMCs) and corroborated some of our findings in lungs and pulmonary arteries of patients with PAH. Both patients with idiopathic PAH and SU/Hx rats had increased expression of lung inflammatory markers and signs of PASMC dedifferentiation in pulmonary arteries. Acetazolamide and NH_4Cl ameliorated SU/Hx-induced pulmonary hypertension and blunted pulmonary and systemic inflammation. Expression of carbonic anhydrase isoform 2 was increased in alveolar macrophages from SU/Hx animals, classically (M1) and alternatively (M2) activated BMDMs, and lungs of patients with PAH. Carbonic anhydrase inhibition and acidosis had distinct effects on M1 and M2 markers in BMDMs. Inflammatory cytokines drove PASMC dedifferentiation, and this was inhibited by acetazolamide and acidosis. The protective antiinflammatory effect of acetazolamide in pulmonary hypertension is mediated by a dual mechanism of macrophage carbonic anhydrase inhibition and systemic metabolic acidosis.

Keywords: acidosis; acetazolamide; macrophages; carbonic anhydrases; lung

(Received in original form July 19, 2018; accepted in final form April 2, 2019)

*These authors contributed equally to this work.

‡S.K. is Associate Editor of *AJRCMB*. Her participation complies with American Thoracic Society requirements for recusal from review and decisions for authored works.

Supported by National Institutes of Health grants R01 HL116573 (H.C.), R01 HL055454 (S.K.), R01 HL114839 (L.E.F.), 5F32HL131228-02 (P.D.), and R24 HL123767 (M.W.G.) and by the Royal College of Surgeons, Dublin, Ireland (N.C.). Funding for the Pulmonary Hypertension Breakthrough Initiative is provided under a National Heart, Lung, and Blood Institute R24 grant (R24 HL123767) and by the Cardiovascular Medical Research and Education Fund. The Boston Children's Hospital Intellectual and Developmental Disabilities Research Center Molecular Genetics Core Facility is supported through National Institutes of Health award P30 HD 18655.

Author Contributions: H.H. and Z.M. participated in study design and execution, data collection, analysis, and manuscript writing. N.C. and E.J.F. participated in study execution, data collection, analysis, and manuscript editing. G.R.W. and A.F.-G. participated in study execution and manuscript writing. R.S.S. and M.W.G. performed the microarray of human tissues and contributed to manuscript writing. P.D. and L.E.F. participated in data collection and analysis and provided input to the manuscript. S.K. provided input to study design, execution, and data analysis and reviewed the manuscript. H.C. contributed to study design, supervision of study execution, manuscript writing, data analysis, and final editing and approval of the manuscript.

Correspondence and requests for reprints should be addressed to Helen Christou, M.D., Department of Pediatric Newborn Medicine, Brigham and Women's Hospital, 75 Francis Street, Thorn 1019, Boston, MA 02115. E-mail: hchristou@bwh.harvard.edu.

This article has a data supplement, which is accessible from this issue's table of contents at www.atsjournals.org.

Am J Respir Cell Mol Biol Vol 61, Iss 4, pp 512–524, Oct 2019

Originally Published in Press as DOI: 10.1165/rcmb.2018-0232OC on April 5, 2019
Internet address: www.atsjournals.org

Clinical Relevance

Pulmonary hypertension is a serious disease in urgent need of effective therapies that will prolong the length and improve the quality of patients' lives. Current therapies target pulmonary vascular tone and have positively impacted the outcome of this disease, but identification of inflammation as a key pathogenetic factor has opened new avenues of investigation into the role of specific therapies that ameliorate inflammation. We report amelioration of pulmonary inflammation and experimental pulmonary hypertension with the use of carbonic anhydrase inhibition and describe a novel role of carbonic anhydrase in macrophage activation and vascular smooth muscle cell dedifferentiation in a preclinical model of severe experimental pulmonary hypertension.

Pulmonary arterial hypertension (PAH) is an often fatal disease characterized by elevated pulmonary artery pressure, progressive right ventricular hypertrophy (RVH) and right ventricular failure. Several pathogenic factors have been described, including genetic predisposition and environmental exposures (1). Despite diverse etiology, PAH is characterized pathologically by disrupted pulmonary vascular cell homeostasis and extensive vasculopathy.

The contribution of inflammation to PAH pathogenesis has been demonstrated in preclinical and human studies (2–10). Elevated circulating concentrations of cytokines are associated with poor outcomes in patients with PAH (5, 8). Moreover, PAH lungs demonstrate characteristic perivascular inflammatory infiltrates containing lymphocytes, mast cells, dendritic cells, and macrophages (4, 6). Preclinical studies employing antiinflammatory approaches have shown promise (11–13), but there is an unmet need to translate these approaches to feasible clinical applications for patients with PAH (14).

Macrophage recruitment and activation (proinflammatory [M1-like] and alternatively activated [M2-like]) play a pivotal pathogenetic role in hypoxia-induced pulmonary hypertension (9, 15) in the mouse and in the Sugen/athymic rat models (13); by convention, experimental pulmonary hypertension is designated as "PH." The potentially causal link between pulmonary inflammation and PAH pathogenesis is incompletely understood but may involve pulmonary artery smooth muscle cell (PASMC) dedifferentiation in response to inflammatory cytokines (12, 16–18). We previously showed that induced metabolic acidosis by ammonium chloride (NH_4Cl) ameliorated PH and restored a contractile PASMC phenotype (19), but the underlying molecular mechanisms were not fully characterized. Given that carbonic anhydrase inhibitors (CAIs) cause metabolic acidosis and that both CAIs and metabolic acidosis were recently shown to have immunomodulatory effects (20–24), we examined whether carbonic anhydrase inhibition and induction of metabolic acidosis exert antiinflammatory and thus beneficial effects in severe experimental PH.

Carbonic anhydrases (CAs) are ubiquitously expressed and catalyze the enzymatic hydration of carbon dioxide to bicarbonate and protons. The 16 known mammalian CA isoforms differ in catalytic activity, subcellular localization, and tissue distribution, and several clinically used drugs have carbonic anhydrase inhibitory activity (25). Ongoing studies are evaluating the therapeutic potential of CAIs in the fields of cancer, obesity, and allergic inflammation (20, 25). Intriguingly, the CAI acetazolamide (ACTZ) has been shown to exert beneficial effects in hypoxic PH (26). However, CAs' role in macrophage activation and PAH has not been studied previously.

In this study, we investigated whether the lung inflammatory response and the hemodynamic and structural components of severe experimental PH can be modulated by ACTZ or NH_4Cl. We also corroborated our findings in human lung samples of patients with PAH, which lends translational support for using CAIs as novel immune modulators in PAH.

Methods

Human Tissues

Samples of human lungs and pulmonary arteries (PAs) were provided by the University of Alabama at Birmingham under the Pulmonary Hypertension Breakthrough Initiative (PHBI). The Partners Human Research Committee approved the present study, and lung tissue collection was approved by the institutional review boards at all lung transplant sites. Patient characteristics are provided in the data supplement (*see* Tables E2 and E3 in the data supplement).

Sugen 5416/Hypoxia Model of PH

PH was induced as previously described (27). Adult (12-wk-old) male Sprague-Dawley rats were given a subcutaneous injection with 20 mg/kg of Sugen 5416 (Sigma-Aldrich) in DMSO (Sigma-Aldrich), placed in hypoxic condition for 3 weeks, and then returned to normoxia (21% O_2). Oxygen was controlled to $9 \pm 0.2\%$ using an OxyCycler controller (BioSpherix). Ventilation was adjusted with a fan and port holes to remove CO_2 and ammonia. Control rats were injected with an equal volume of vehicle (DMSO) in normoxic condition. The endpoints of the study were 24 or 49 days after injection.

Human Microarray Analysis

A total of 83 lung samples from 58 patients with PAH and 25 control lung failed donors (FDs) were analyzed by Affymetrix GeneChip Human Gene 1.0 ST microarray analysis. The .cel files were imported into Partek Genomics Suite (6.6) (http://www.partek.com/partek-genomics-suite/), and an ANOVA model was used to identify differentially regulated genes between the PAH and FD lung transcriptomes after correcting for batch and sex imbalance. Batch effects were derived from the microarrays being processed over three successive years owing to slow patient recruitment. Sex imbalance within PAH (lung tissues were ~3:1 female/male, as expected for PAH) was further exacerbated by FD tissue acquisition (1:2 female/male; $P = 0.0002$ by χ^2 test for sex imbalance within the microarray study). Differentially expressed genes were identified using a false discovery rate q value less than 0.001, yielding 1,140 significant Affymetrix transcript identifiers (28). Microarray raw data and/or processed data files may be obtained through the PHBI upon request (mgrants.michr.med.umich.edu). Area-proportional Venn diagrams were generated using BioVenn (biovenn.nl).

Statistical Analysis

Statistical analyses were performed using Prism version 5.03 software (GraphPad

Software). We used one-way ANOVA with Tukey's post test (when comparing multiple groups) or Student's *t* test (when comparing two groups). When numbers permitted, we used the D'Agostino-Pearson omnibus normality test, and data with non-Gaussian distribution were analyzed by Kruskal-Wallis test with Dunn's post test or Mann-Whitney *U* test. Correlation of lung Il6 expression with Fulton's index (FI) was analyzed by nonparametric Spearman's test. Linear regression was performed for different groups to assess the statistical significance of slope differences. Data are presented as individual data points and mean with SD or mean with SEM. Individual statistical tests are described in the corresponding figure legends. *P* values less than 0.05 were considered statistically significant.

Results

Treatment with ACTZ or NH_4Cl Ameliorates SU/Hx-induced PH

In an early intervention protocol (Figure 1A), treatment started in the drinking water on Day 7 and ended on Day 24 after SU/Hx-induced PH. Both ACTZ and NH_4Cl induced metabolic acidosis, as seen by blood gas analysis (Table E1). Both interventions significantly decreased right ventricular systolic pressure and mean pulmonary artery pressure (Figures 1B–1D) without significantly affecting left ventricular systolic pressure (Figure 1E) and reduced RVH, as assessed by FI and ratio of right ventricular to total body weight (Figures 1F–1H).

ACTZ treatment also reversed established PH in a late intervention protocol (treatment from Day 28 to Day 49 after SU/Hx-induced PH) (Figure 2A). ACTZ treatment induced mild metabolic acidosis (Table E1) and ameliorated right ventricular systolic pressure (Figures 2B and 2C) without significantly affecting left ventricular systolic pressure (Figure 2D). Also, RVH was ameliorated, as seen by lower FI and ratio of right ventricular to total body weight (Figures 2E and 2F). Overall, the degree of protection was less than with the early intervention protocol. Histology of peripheral lung sections at 7 weeks after SU/Hx-induced PH showed an increase in percentage wall thickness of arterioles less than 100 μm in diameter in SU/Hx animals and amelioration of vascular remodeling in the ACTZ treatment group (Figures 2G and 2H). Occlusive lesions, known to occur at 13–14 weeks after SU/Hx-induced PH (27), were not observed in our animals.

ACTZ and NH_4Cl Dampen Pulmonary and Systemic Inflammation in SU/Hx Model

Whole-lung mRNA concentrations of proinflammatory mediators (Tnf, Il6, and Ccl2) were significantly increased in SU/Hx animals on Day 24 and were decreased to baseline by both interventions in the early intervention protocol (Figure 3A). Whole-lung Il6 mRNA concentrations correlated with RVH severity (expressed as FI) (Figure 3B). Plasma Il6 concentrations were significantly higher in SU/Hx animals than in control animals, and treatment with ACTZ or NH_4Cl reduced these concentrations to baseline (Figure 3C). Human idiopathic pulmonary arterial hypertension (IPAH) lung samples showed a similar induction for IL-6 and CCL2 and upregulation of IL-1β mRNA (Figure 3D) compared with FD lung samples (*see* Table E3 for patient information from PHBI).

Proinflammatory Mediators Promote PASMC Dedifferentiation, and This Is Inhibited by ACTZ or Metabolic Acidosis

Primary rat PASMCs were exposed to 10 ng/ml TNF-α or IL-1β for 24 hours, and this resulted in downregulation of the mRNA of the transcriptional coactivator myocardin (Myocd) and of multiple markers of a contractile vascular smooth muscle cell (VSMC) phenotype (Tagln [transgelin], Smtn [smoothelin], Acta2, Cnn1 [calponin 1], and Myh11 [myosin heavy chain 11]), as well as increased mRNA for markers of dedifferentiation (Rbp1 [retinol-binding protein 1]) and proliferation (Ccnd1 [cyclin D1]) (Figures 3E and 3F). PASMCs exposed to TNF-α also displayed altered morphology (Figure E1A) and increased proliferation in response to 20% FBS, which was significantly inhibited by exposure to ACTZ or acidosis (Figures E1B and E1C). Treatment with ACTZ or exposure to metabolic acidosis also restored the mRNA concentrations of Myocd and of the contractile markers Smtn, Acta2, Tagln, Cnn1, and Myh11 in TNF-α–treated PASMCs (Figure E1D).

Dedifferentiation of PASMCs in IPAH and Effect of ACTZ in SU/Hx Model

As shown in Figure 4A, we found that all contractile markers were downregulated in PAs from patients with IPAH compared with control subjects and that statistical significance was reached for MYOCD, TAGLN, and CNN1. Expression of the proliferative marker CCND1 was higher in IPAH PAs than in controls, whereas the expression of the dedifferentiation marker RBP1 was unchanged. PAs harvested from SU/Hx-treated rats showed the same pattern of dedifferentiation compared to PAs from control animals with decreased contractile and increased proliferative markers (Figure 4B). Treatment of SU/Hx animals with ACTZ (early intervention protocol) partially restored mRNA concentrations of the contractile markers Myocd, Tagln, Smtn, and Acta2 and reduced concentrations of the proliferative marker Ccnd1 (Figure 4B) in their PAs. Importantly, PASMCs from control, SU/Hx-treated, and ACTZ-treated animals retained their respective phenotypes *in vitro*. (No ACTZ was used in culture media.) After passage 1 and 48 hours of serum deprivation (0.5% FBS), PASMCs of SU/Hx-treated rats but not those of ACTZ-treated rats showed dedifferentiation across the entire panel of markers (Figure 4C) and no baseline differences in proliferation. (Ccnd1 expression was unchanged; data not shown.) When stimulated with 20% FBS, PASMCs of SU/Hx-treated rats showed a significantly higher rate of proliferation than those from healthy animals, whereas PASMCs from ACTZ-treated animals proliferated at a rate similar to those from healthy animals (Figure 4D).

ACTZ Modulates Alveolar Macrophage Activation Profile in SU/Hx Model of PH

Given that alveolar macrophages (AMs) were previously implicated in PH pathogenesis (9), we examined AM activation in the SU/Hx model and evaluated the effect of our interventions. AMs were isolated from BAL from our experimental animals, and their purity was confirmed by flow cytometry and cytospin (Figures 5A and 5B). AMs of SU/Hx-treated animals showed significant upregulation of proinflammatory markers similar to that seen in whole

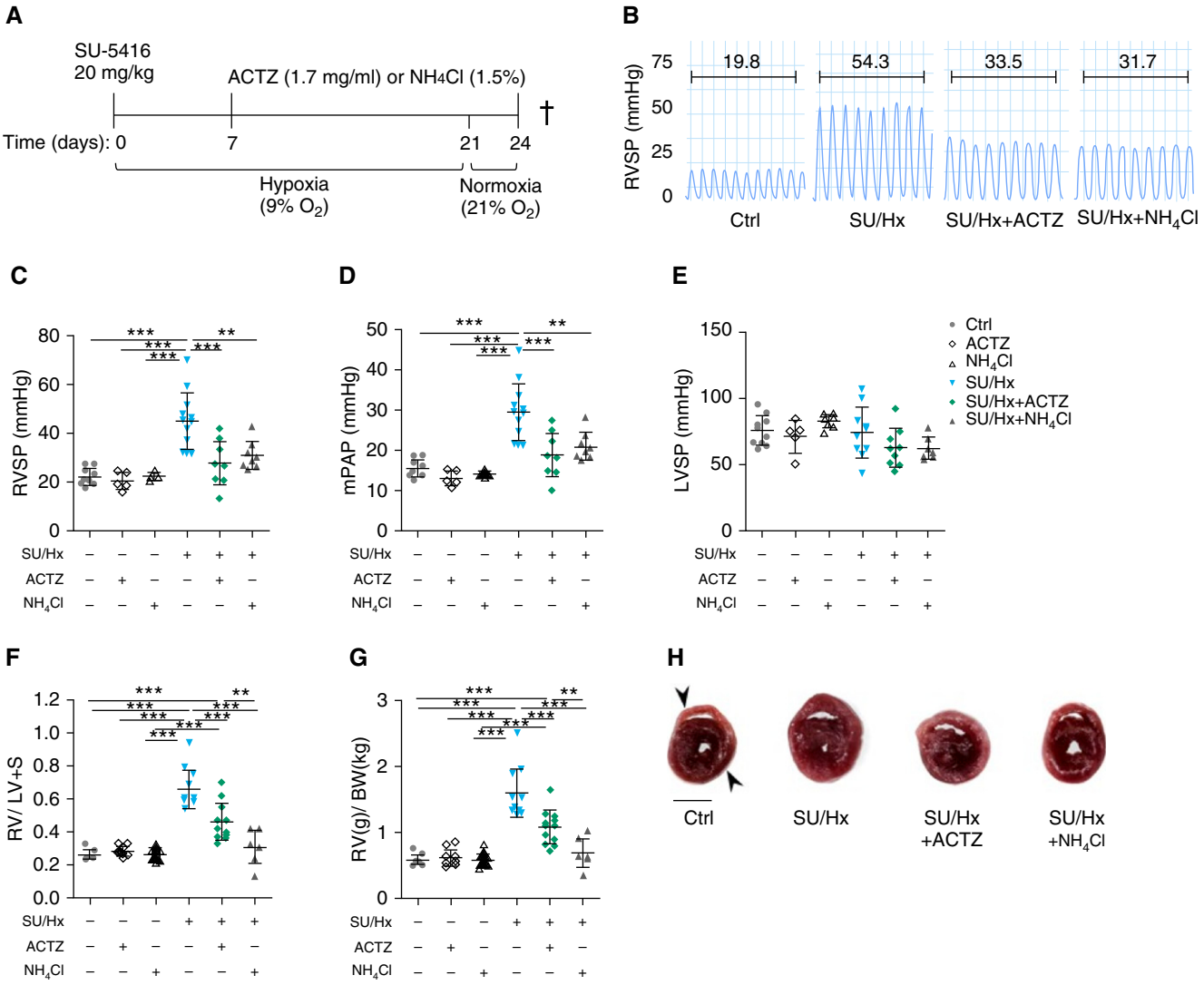

Figure 1. Early treatment with acetazolamide (ACTZ) or ammonium chloride (NH_4Cl) ameliorates Sugen 5416/hypoxia (SU/Hx)-induced pulmonary hypertension. (*A*) Experimental timeline, early intervention. Rats were administered an injection with Sugen 5416 (SU; 20 mg/kg s.c.) and housed under hypoxic condition (9% O_2) for 3 weeks followed by 3 days under normoxic condition (21% O_2). Treatment was administered with ACTZ (1.7 mg/ml) or NH_4Cl (1.5%) *ad libitum* in the drinking water from Day 7 to Day 24. Control rats were treated with either ACTZ or NH_4Cl in normoxia for the same time period. †This represents the study endpoint when the animals were killed. (*B*) Representative right ventricular pressure tracings measured on Day 24 and corresponding mean right ventricular systolic pressure (RVSP) in millimeters of mercury. Experimental groups: vehicle-injected normoxic controls (Ctrl), ACTZ- or NH_4Cl-treated normoxic controls (ACTZ or NH_4Cl), SU/Hx and ACTZ- or NH_4Cl-treated SU/Hx animals (SU/Hx + ACTZ and SU/Hx + NH_4Cl). (*C* and *D*) ACTZ and NH_4Cl treatment significantly decreased RVSP and mean pulmonary artery pressure (mPAP). $n = 8$–21 rats per group. (*E*) Both interventions had no significant effect on left ventricular systolic pressure (LVSP). $n = 8$–10 rats per group. (*F* and *G*) Right ventricular hypertrophy is significantly ameliorated by both interventions. Right ventricular hypertrophy was assessed by Fulton's index (ratio of right ventricular weight to left ventricular + septal [S] weight) (*F*) and as the ratio of right ventricular weight to total body weight (RV/BW) (*G*). $n = 7$–23 per group. (*H*) Representative transverse cross-sections at midpapillary level from the four experimental groups. Right ventricle is indicated by upper arrowhead and left ventricle by lower arrowhead. Scale bar: 5 mm. Statistical analysis by one-way ANOVA and Tukey's *post hoc* test. Error bars are mean ± SD (**$P < 0.01$ and ***$P < 0.001$). s.c. = subcutaneous.

lung (Tnf, Il6, Ccl2), and treatment with either ACTZ or NH_4Cl completely suppressed this upregulation (Figure 5C). Furthermore, AMs of SU/Hx-treated animals displayed higher expression of markers of alternative activation, including Ccl17 and Arg1 (arginase 1), and this was blunted by ACTZ treatment (Figure 5D). In contrast, NH_4Cl treatment had no effect on Ccl17 mRNA induction in SU/Hx AMs and significantly increased Arg1 mRNA (Figure 5D). The same pattern of M2 marker induction in SU/Hx-treated animals and suppression by ACTZ treatment was recapitulated in whole-lung mRNA analysis (Figure 5E). Again, NH_4Cl treatment was less effective than ACTZ in suppressing markers of alternative macrophage activation in whole lungs of SU/Hx-treated animals. Interestingly, the baseline state of activation of bone marrow–derived macrophages (BMDMs) from control, diseased, and treated animals was not different (data not shown).

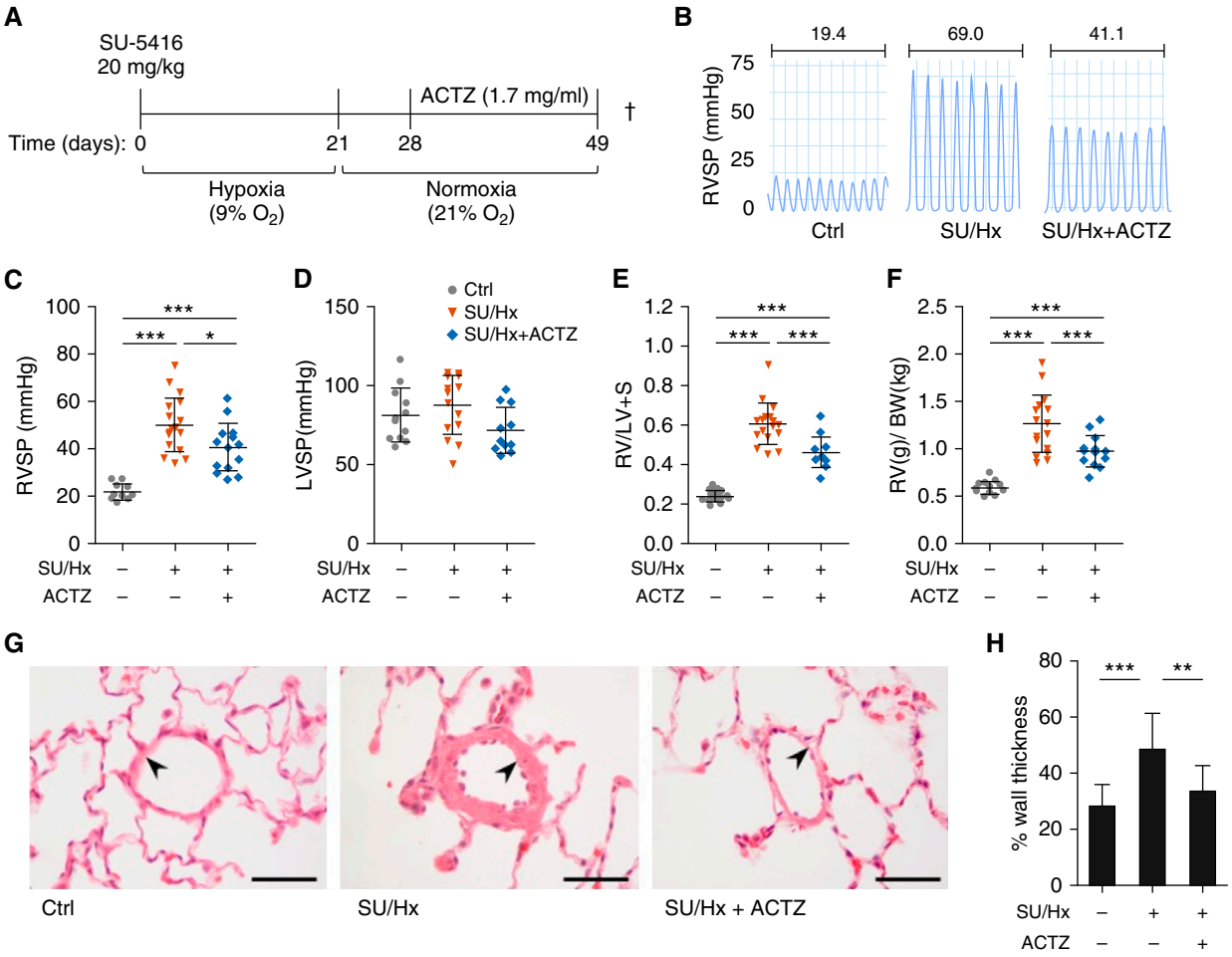

Figure 2. Late treatment with ACTZ partially reverses SU/Hx-induced pulmonary hypertension. (*A*) Experimental timeline, reversal. Rats were administered injections with SU 5416 (20 mg/kg s.c.) and housed under hypoxic condition (9% O_2) for 3 weeks followed by 4 weeks in normoxic condition (21% O_2). Treatment was administered with ACTZ (1.7 mg/ml) *ad libitum* in the drinking water from Day 28 to Day 49. †This represents the study endpoint when the animals were killed. (*B*) Representative right ventricular pressure tracings measured on Day 49 and corresponding mean RVSP in millimeters of mercury. Experimental groups: vehicle-injected normoxic controls (Ctrl), SU/Hx- and ACTZ-treated animals (SU/Hx + ACTZ). (*C*) ACTZ treatment partially reversed established elevation in RVSP. $n = 10$–18 rats per group. (*D*) ACTZ treatment had no significant effect on LVSP. $n = 10$–15 rats per group. (*E* and *F*) ACTZ treatment partially reversed right ventricular hypertrophy. Right ventricular hypertrophy was assessed by Fulton's index (*E*) and ratio of RV/BW (*F*). $n = 13$–18 per group. (*G*) Pulmonary vascular remodeling is ameliorated by treatment with ACTZ. Representative images of pulmonary arterioles on hematoxylin and eosin–stained lung sections of Ctrl animals, SU/Hx animals, and SU/Hx animals treated with ACTZ (late intervention, Days 28–49). Scale bars: 50 μm. Arterioles are indicated by arrowheads. (*H*) Morphometric analysis of pulmonary vascular remodeling assessed by percentage wall thickness. $n = 23$–40 arterioles (diameter, 50–100 μm) from $n = 5$ animals per group. Data are presented as mean ± SD. Statistical analysis by Kruskal-Wallis test and Dunn's *post hoc* test. (*C*–*F*) Error bars are mean ± SD. Statistical analysis by one-way ANOVA and Tukey's *post hoc* test (*$P < 0.05$, **$P < 0.01$, and ***$P < 0.001$).

AM Supernatants and ACTZ Treatment Modulate PASMC Phenotype

To evaluate whether secreted mediators from AMs drive changes in PASMC differentiation, we incubated AMs from experimental animals for 24 hours, collected conditioned media (CM), and added them to PASMCs in culture for 24 hours (Figure 5F). Media alone (not exposed to AM) and 5 ng/ml TNF-α served as negative and positive controls, respectively. Compared with AM-CM from control animals, AM-CM from SU/Hx-treated animals promoted PASMC dedifferentiation, as seen by significantly decreased contractile and increased synthetic and proliferative markers (Figure 5G). Interestingly, mRNA concentrations of all PASMC markers tested were unchanged after exposure to AM-CM from ACTZ-treated animals. In contrast, AM-CM from NH_4Cl-treated animals only partially ameliorated PASMC dedifferentiation compared with AM-CM from SU/Hx-treated animals (Figure 5G).

Metabolic Acidosis Modulates Macrophage Polarization

We evaluated the distinct effect of acidosis and CAIs on macrophage activation using BMDMs from healthy rats. BMDMs were polarized to a classically activated M1 (LPS and IFN-γ) or an alternatively activated M2 (IL-4 and IL-13) phenotype (Figure 6A). Metabolic acidosis suppressed M1 polarization in a pH-dependent manner, as indicated by decreased Tnf, Il6, and Ccl2 mRNA concentrations (Figure E2A)

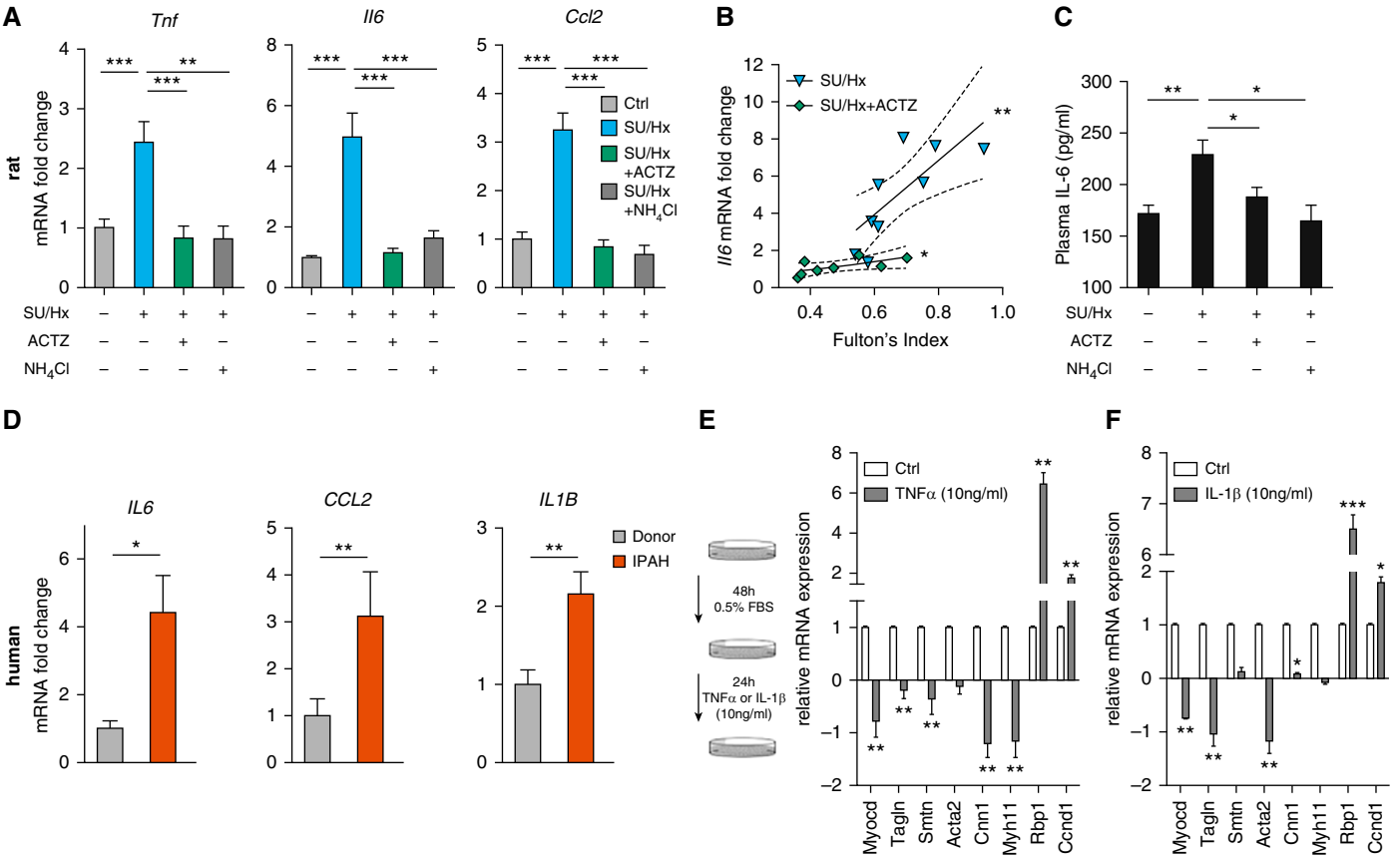

Figure 3. Early treatment with ACTZ or NH_4Cl dampens the pulmonary and systemic inflammatory response in SU/Hx-induced pulmonary hypertension. (*A*) Significantly increased mRNA levels of the proinflammatory mediators Tnf, Il6, and Ccl2 in whole lungs from SU/Hx animals were seen on Day 24, and treatment with ACTZ or NH_4Cl significantly decreased their expression. Data are expressed as mRNA fold change with Ctrl set as 1. $n = 5$–12 animals per experimental group from the early intervention protocol. Data are presented as mean ± SEM. Statistical analysis by one-way ANOVA and Tukey's *post hoc* test. (*B*) Pulmonary Il6 expression significantly correlated with right ventricular hypertrophy severity, expressed as Fulton's index in SU/Hx (**) animals and in SU/Hx animals treated with ACTZ (*). Statistical analysis by Spearman's test. The linear regressions between the two groups (SU/Hx, $r^2 = 0.56$; SU/Hx + ACTZ, $r^2 = 0.51$) differ significantly (*). Data are presented as mRNA fold change (from *A*) versus Fulton's index with linear regression (solid line) and 95% confidence interval (dashed line). (*C*) Circulating plasma IL-6 is elevated in SU/Hx rats, and both ACTZ and NH_4Cl treatments decrease IL-6 levels to baseline. IL-6 concentration in pg/ml was measured in plasma by ELISA. $n = 3$–8 animals per experimental group. Data are presented as mean ± SEM. Statistical analysis by one-way ANOVA and Tukey's *post hoc* test. (*D*) Expression of proinflammatory mediators was upregulated in lungs from patients with idiopathic pulmonary arterial hypertension (IPAH) compared with failed donor lungs (Donor; set as 1). $n = 12$ patients per group (6 male and 6 female, age matched to ±1 yr). Statistical analysis by Mann-Whitney *U* test. (*E* and *F*) TNF-α treatment (*E*) and IL-1β treatment (*F*) lead to pulmonary artery smooth muscle cell (PASMC) dedifferentiation *in vitro*. Rat pulmonary artery smooth muscle cells were serum deprived (0.5% FBS) for 48 hours followed by stimulation with 10 ng/ml rat TNF-α or IL-1β for 24 hours. Relative mRNA expression of genes associated with the contractile apparatus of smooth muscle was compared with untreated controls set as 1. Markers were either regulatory (Myocd), contractile (Tagln, Smtn, Acta2, Cnn1, Myh11), synthetic (Rbp1), or proliferative (CCND1). Data represent mean ± SEM from $n = 3$–6 independent experiments. Statistical analysis by Student's *t* test (*$P < 0.05$, **$P < 0.01$, and ***$P < 0.001$).

and decreased TNF-α and IL-6 protein concentrations in culture supernatants (Figure E2C). Furthermore, acidosis promoted M2 polarization of BMDMs, as shown by increased Ccl17, Arg1, and Cd163 mRNA concentrations (Figure E2B). Interestingly M1 polarization was associated with significantly higher concentrations of the proton sensor Gpr65 (G protein–coupled receptor 65) mRNA compared with M0 and M2 BMDMs (Figure E2D).

Increased Carbonic Anhydrase 2 Expression during Macrophage Polarization and Modulating Effect of Carbonic Anhydrase Inhibition

Among the CA isoforms known to be expressed in macrophages, carbonic anhydrase 2 (Car2) was the most abundant in M0 as well as M1- and M2-polarized BMDMs (Figure 6B). Furthermore, M1 and M2 polarization were accompanied by marked upregulation of Car2 mRNA and protein (Figures 6C, 6D, and E3B), and ACTZ suppressed M1 activation in a dose-dependent manner (Figure 6E). Ethoxzolamide (EZA), a CAI with high affinity to Car2, similarly suppressed M1 activation of BMDMs (Figure 6F). Both ACTZ and EZA also inhibited the secretion of TNF-α and IL-6 in supernatants (Figure 6G). In addition, both ACTZ and EZA suppressed M2 polarization as assessed by Ccl17, Arg1, and Cd163 mRNA concentrations (Figure 6H).

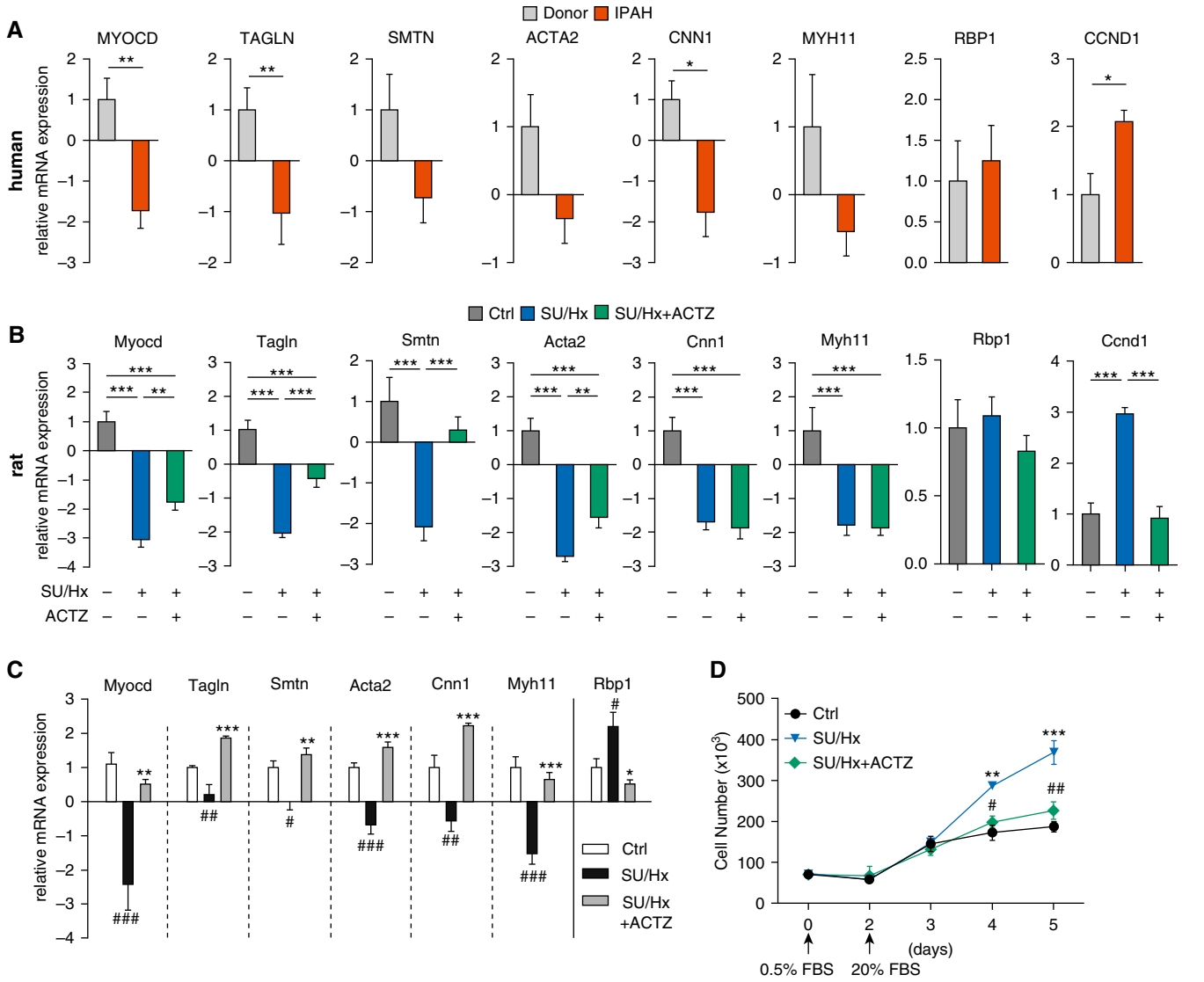

Figure 4. ACTZ treatment partially restores PASMC phenotype in the SU/Hx model. (*A*) Relative expression of PASMC markers representative of a contractile (MYOCD, TAGLN, SMTN, ACTA2, CNN1, MYH11), synthetic (RBP1), and proliferative (CCND1) phenotype in pulmonary arteries from patients with IPAH compared with failed donor control pulmonary arteries (Donor; set as 1). $n = 13$ donor samples (10 male, 3 female) and $n = 10$ IPAH samples (6 male, 4 female). Statistical analysis by Mann-Whitney *U* test. (*B*) Vascular smooth muscle cell markers in pulmonary artery samples from SU/Hx rats showed a similar pattern of dedifferentiation expression profiles seen in human IPAH. Significant reduction in all contractile markers in SU/Hx animals compared with Ctrl and partial reversal by ACTZ treatment. Upregulation of CCND1 is ameliorated by ACTZ treatment. $n = 9$–15 per experimental group. Statistical analysis by one-way ANOVA and Tukey's *post hoc* test. (*C*) Primary PASMCs from control, SU/Hx, and SU/Hx + ACTZ animals retained their phenotype *in vitro*. PASMCs at passage 1 were grown to subconfluence and kept in 0.5% FBS for 48 hours. $n = 3$–8 cell cultures per group. Significant differences from control (#) and SU/Hx (*) are noted. (*D*) PASMCs from SU/Hx animals showed a higher rate of proliferation than PASMCs from control or SU/Hx + ACTZ animals. Proliferation was induced after 48 hours in 0.5% FBS by media supplemented with 20% FBS, and cell numbers were determined. $n = 6$ cell cultures per group. Significant differences on Days 4 and 5 between control and SU/Hx (*) and SU/Hx + ACTZ and SU/Hx (#) are indicated. (*A–D*) Data are presented as mean ± SEM. (*C* and *D*) Statistical analysis by one-way ANOVA and Tukey's *post hoc* test ($^{*}P < 0.05$, $^{**}P < 0.01$, $^{***}P < 0.001$, $^{\#}P < 0.05$, $^{\#\#}P < 0.01$, and $^{\#\#\#}P < 0.001$).

Car2 Is Upregulated in AMs in SU/Hx Model and in Human PAH Lungs

AMs from control animals showed abundant amounts of Car2 mRNA and protein, and the expression was significantly increased in AMs from SU/Hx-treated animals compared with control animals (Figures 7A–7C and E3C). Lending support to the clinical relevance of this observation, in a large gene array of 58 subjects with PAH and 25 FD specimens, CA2 was one of the 279 most dysregulated (>1.5-fold up- or downregulated) genes in human PAH lung (Figure 7D). We confirmed upregulation of CA2 mRNA in a cohort of IPAH lung samples compared with donor lung samples (Figure 7E).

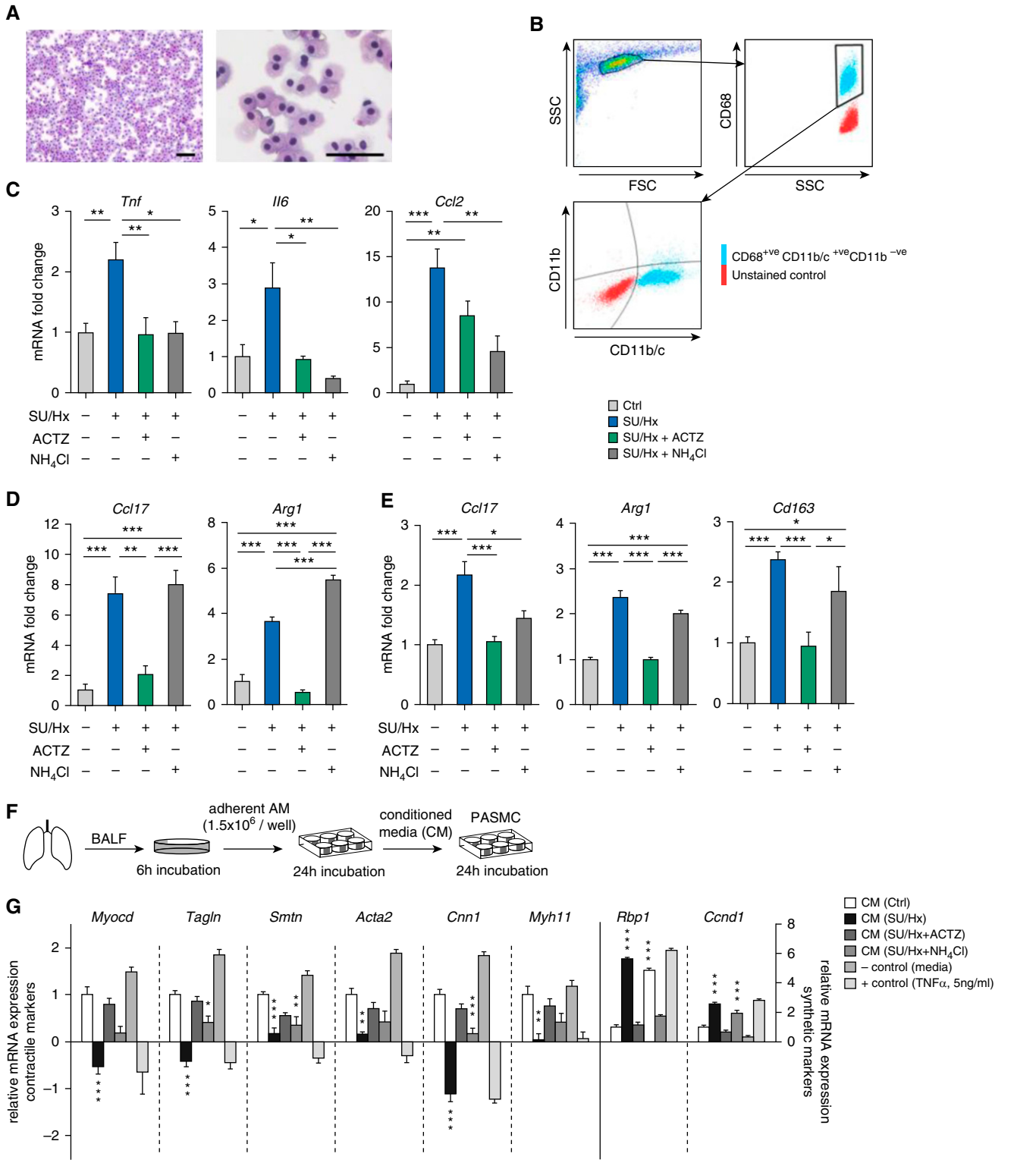

Figure 5. ACTZ alters the activation profile of alveolar macrophages (AMs) in the SU/Hx model. (*A*) Representative cytospin images of BAL after 6 hours of adherence to tissue culture dishes (>99% of cells are AMs). Scale bars: 50 μm. (*B*) Flow cytometric analysis of AM-enriched BAL showed a highly pure cell population positive for Cd68 and Cd11c (>99% $Cd68^{+}$; >90% $Cd11b/c^{+}$; <10% $Cd11b^{+}$). (*C* and *D*) AMs from SU/Hx animals showed upregulated expression of markers associated with proinflammatory (Tnf, Il6, and Ccl2) (*C*) and alternatively activated (Ccl17 and Arg1) (*D*) macrophages. ACTZ and NH_4Cl both suppress proinflammatory activation, but only ACTZ modulates markers of alternative activation. $n = 4–7$ animals per experimental group. (*E*) Whole-lung gene expression showed a similar pattern of suppression of markers associated with alternative macrophage activation by ACTZ but not by

Discussion

We report amelioration of pulmonary inflammation and improvement in SU/Hx-induced experimental PH by two different interventions that induce metabolic acidosis (ACTZ and NH_4Cl). We further demonstrate that CA inhibition and metabolic acidosis have distinct effects in macrophage activation and suggest a novel role for CAs in macrophage function.

Our results are in agreement with those of a prior study (26) that reported amelioration of hypoxic PH with ACTZ treatment, and they build on our earlier studies in which NH_4Cl treatment attenuated both hypoxic and monocrotaline-induced PH (19). In line with a previous study of SU/Hx-induced PH (29), we found increased lung concentrations of Tnf, Il6, and Ccl2 mRNA and elevated circulating concentrations of IL-6. These findings were ameliorated by both ACTZ and NH_4Cl treatments. Similarly, we found increased concentrations of IL-6, CCL2, and IL-1β mRNA in lung specimens of patients with IPAH compared with donor control subjects, and this is in agreement with prior studies in which circulating proinflammatory cytokines such as IL-6 and TNF-α were elevated and partially predicted outcomes in patients with PAH (5). The contribution of inflammation was also described in preclinical models of PH (9, 12, 29, 30). Although causality is difficult to prove, some inflammatory mediators, such as IL-6, are accepted to contribute to disease progression (7), and pharmacological targeting of the IL-6 receptor or TNF-α ameliorates experimental PH (11, 12). However, trials on immune modulators in PAH have yielded conflicting results, and new targeted approaches are urgently needed (14).

The role of macrophages in mediating inflammation and vascular remodeling in hypoxic PH is supported by prior studies (2). Early recruitment and alternative activation of macrophages are critical for hypoxic PH (9) in the mouse, and AMs are essential in translating alveolar hypoxia into a systemic inflammatory response, as seen in PH (31). Also, specific targeting of pulmonary macrophages may ameliorate experimental PH (13). We report that AMs in the SU/Hx rat model display upregulated markers of both proinflammatory and alternative activation, which is in agreement with the concept of a continuum in macrophage activation as opposed to a dichotomous paradigm (14). To our knowledge, we are the first to report that AMs in SU/Hx-induced PH show upregulation of the highly abundant Car2. Intriguingly, we also found CA2 mRNA upregulation in a large human whole-lung microarray analysis of patients with PAH compared with donor control subjects. Using *in vitro* macrophage polarization assays as a proof of concept, we found that both M1 and M2 polarization are associated with significant induction of Car2.

CAs have been implicated in immune cell homeostasis (20, 32). Wen and colleagues showed that eosinophil activation was associated with Car4 upregulation (32), and Henry and colleagues reported that Car1 inhibition in mast cells inhibited type 2 allergic inflammation (20). We now report a previously unrecognized immune-modulatory effect of ACTZ on AMs *in vivo*, suppressing both proinflammatory and alternative activation. We further show that inhibition of CA activity by different CAIs suppresses both M1 and M2 activation *in vitro*. Activated macrophages have high energy demands and increased CO_2 production. CAs have an essential metabolic regulatory role by catalyzing the conversion of CO_2 and H_2O to H_2CO_3, thereby facilitating CO_2 removal. In the setting of CA inhibition, macrophages may be forced to shut down the metabolic machinery for activation, and carbonic anhydrase inhibition might therefore drive metabolic reprogramming, which has been proposed to regulate macrophage polarization (33).

Through inhibition of Car2 and Car4 in the proximal convoluted tubule, ACTZ decreases bicarbonate reabsorption and causes metabolic acidosis. Because metabolic acidosis was previously shown to suppress inflammation through different metabolites, such as lactic acid, ketone bodies, or H^+ (21, 23, 24), we asked whether ACTZ might exert its immune-modulatory effects through metabolic acidosis. Treatment with ACTZ or NH_4Cl induced metabolic acidosis, and BAL-derived AMs in both intervention groups displayed suppression of proinflammatory activation. Interestingly, NH_4Cl failed to suppress markers of alternative activation. BMDMs were used in culture as a proof of concept, and this differential effect of acidosis on proinflammatory and alternative macrophage polarization was recapitulated in *in vitro* assays. Our findings are supported by previous studies showing suppression of proinflammatory activation by acidosis mediated through Gpr65 in peritoneal macrophages (24), which is upregulated upon M1 but not M2 activation (Figure E2D). Furthermore, proinflammatory activation of tumor-associated macrophages is suppressed by lactic acidosis, whereas alternative activation is enhanced (23). We conclude that although both interventions might exert antiinflammatory effects partially through acidosis, suppression of alternative activation as seen in AMs from ACTZ-treated animals may be due at least in part to inhibition of AM CAs.

The link between inflammation and PAH is a subject of intense investigation, but there is sufficient preclinical evidence supporting inflammatory mediators as contributing to VSMC phenotypic switching, a known contributor to PAH pathobiology (16–18). In line with previous studies (34, 35), we found changes in mRNA markers suggestive of VSMC dedifferentiation in isolated PAs of rats

Figure 5. (Continued). NH_4Cl treatment. $n = 5$–11 animals per experimental group. (*F* and *G*) PASMCs were exposed to AM-conditioned media (CM) from the four experimental groups (as outlined in *F*). Effect of CM from SU/Hx animals on PASMC dedifferentiation as assessed by marker expression (black bars) and effect of *in vivo* treatment with ACTZ and NH_4Cl. Asterisks indicate significant differences compared with control (white bar). Media alone served as a negative control (−control), and 5 ng/ml TNF-α served as a positive control (+control). $n = 6$ independent experiments. Data are presented as mean ± SEM. Statistical analysis by one-way ANOVA and Tukey's *post hoc* test (*$P < 0.05$, **$P < 0.01$, and ***$P < 0.001$). BALF = BAL fluid; FSC = forward scatter; SSC = side scatter.

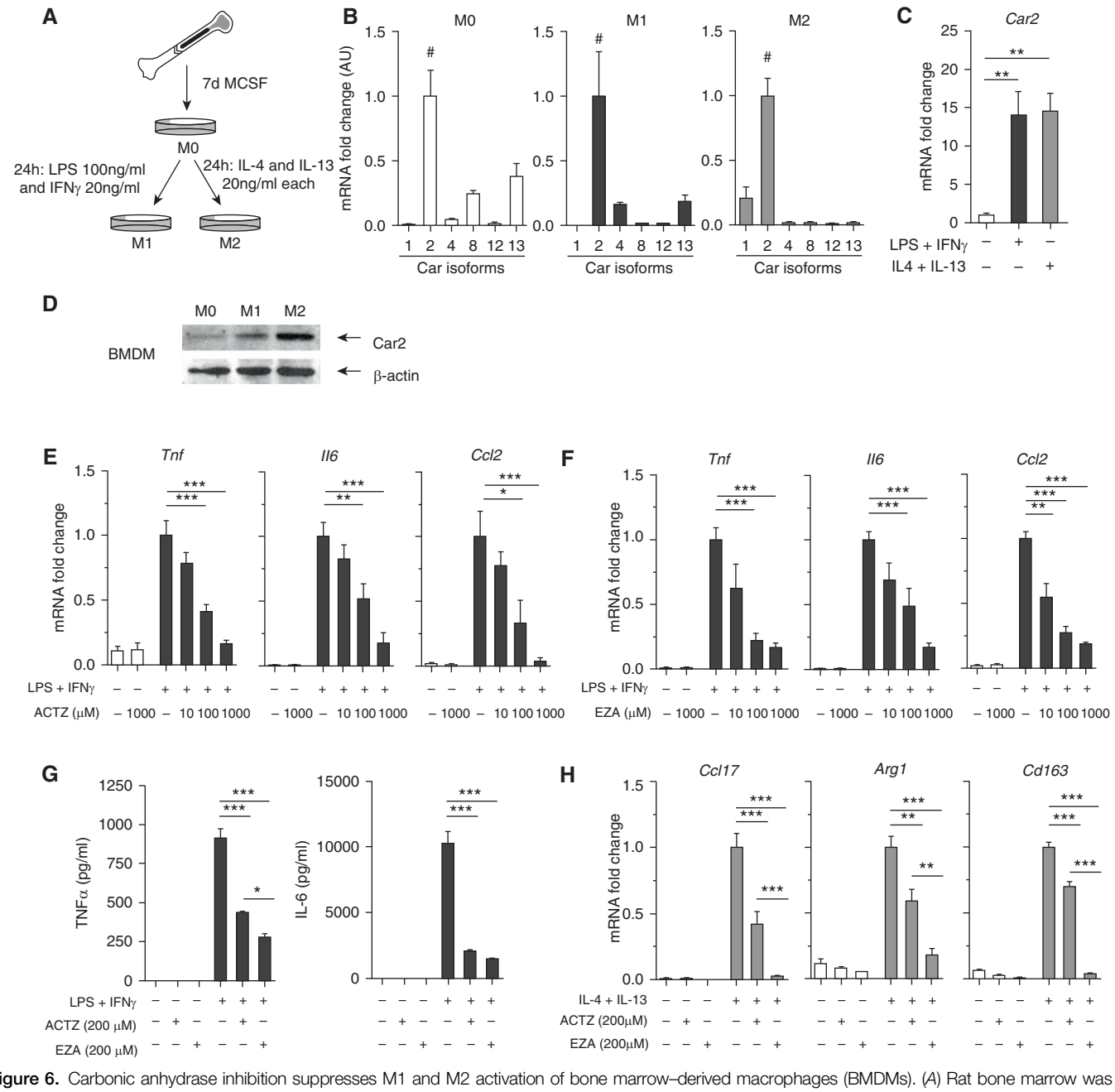

Figure 6. Carbonic anhydrase inhibition suppresses M1 and M2 activation of bone marrow–derived macrophages (BMDMs). (*A*) Rat bone marrow was harvested, and cells were grown in the presence of macrophage colony-stimulating factor for 7 days. BMDMs were polarized toward M1 with LPS and IFN-γ or M2 with IL-4 and IL-13 for 24 hours. Untreated BMDMs were considered M0. (*B*) Expression of different carbonic anhydrase isoforms was assessed by qPCR (Car2 expression is set as 1). Carbonic anhydrase 2 (*Car2*) was the most abundant isoform in M0, M1, and M2 BMDMs (indicated by #). (*C* and *D*) Car2 is significantly upregulated in both M1- and M2-polarized BMDMs compared with M0 at both mRNA (*C*) and protein levels (representative Western blot shown in *D*). Quantification of four independent experiments in Figure E3A. (*E*) ACTZ suppresses M1 activation (Tnf, Il6, and Ccl2) of BMDMs in a dose-dependent manner. (*F*) Ethoxzolamide (EZA) suppresses M1 activation (Tnf, Il6, and Ccl2) of BMDMs in a dose-dependent manner. (*G*) ACTZ and EZA significantly reduce TNF-α and IL-6 secretion by M1-polarized BMDMs, measured by ELISA in cell culture supernatants. No detectable TNF-α or IL-6 in M0 control macrophage supernatants. (*H*) ACTZ and EZA suppress M2 activation (Ccl17, Arg1, and Cd163) of BMDMs. (*B–H*) Data represent mean ± SEM from three or four independent experiments. Statistical analysis by one-way ANOVA and Tukey's *post hoc* test (*$P < 0.05$, **$P < 0.01$, and ***$P < 0.001$).

with SU/Hx-induced PH and humans with IPAH compared with controls. Treatment of primary PASMCs with TNF-α and IL-1β led to suppression of contractile markers and increased proliferation, as was shown before (12, 36, 37).

As we previously reported, acidosis exerts direct effects on PASMC homeostasis by inhibiting the proliferative and migratory response to growth factors and increasing susceptibility to apoptosis (38). We now demonstrate that both acidosis

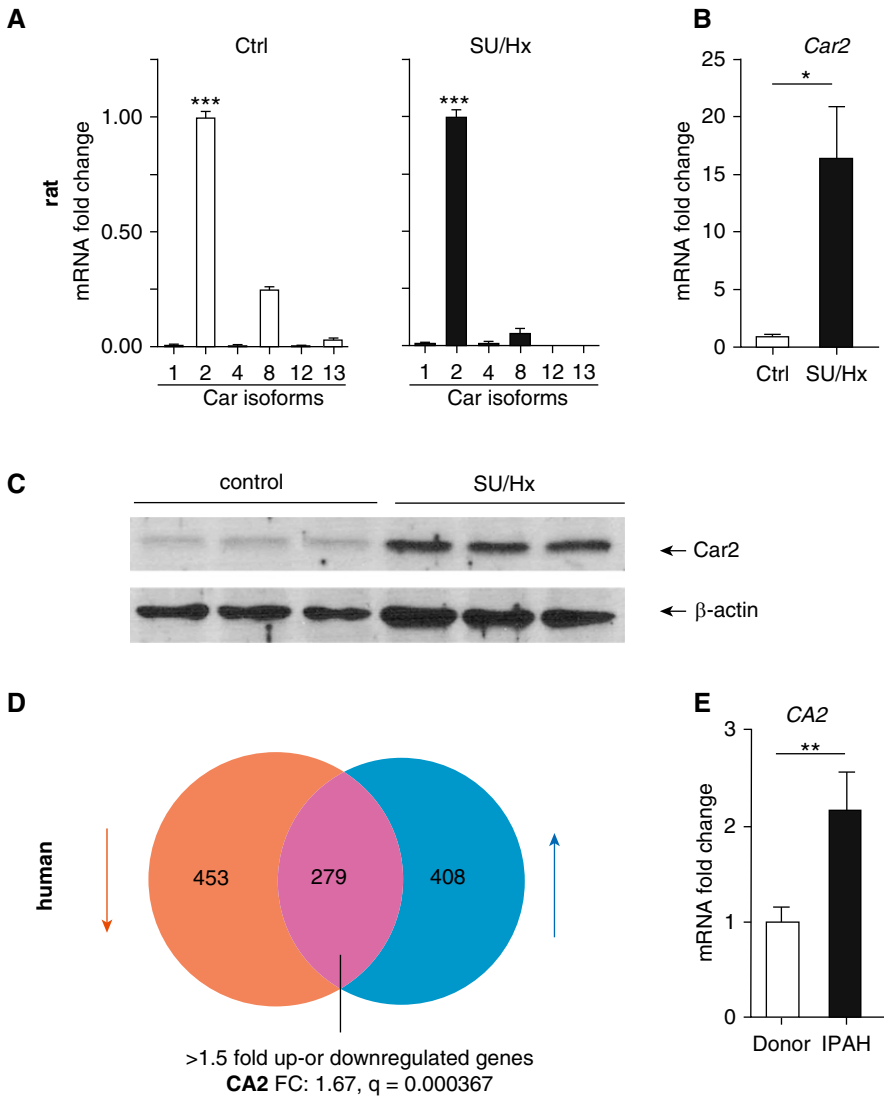

Figure 7. Car2 is upregulated in AMs of SU/Hx rats and in IPAH lungs. (*A*) Expression of different carbonic anhydrase isoforms was assessed in AMs from control and SU/Hx animals (Car2 expression is set as 1). Car2 was by far the most abundant isoform. Statistical analysis by one-way ANOVA and Tukey's *post hoc* test. ***Significant difference from all other groups. (*B*) Car2 is upregulated in AMs from SU/Hx animals compared with control. $n = 4$ animals per group. Statistical analysis by Mann-Whitney *U* test. (*C*) Western blots show increased Car2 enzyme in AMs of SU/Hx animals. Each lane represents AMs from a different animal (quantification in Figure E3B). (*D*) Venn diagram of 1,140 genes that are differentially expressed between PAH and control (failed donor) lungs assessed by Affymetrix gene array (Affy Human Gene ST1.0). $n = 58$ PAH patient and $n = 25$ failed donor lungs. Upregulated genes are shown in blue and downregulated genes in red. Expression of 279 genes was greater than 1.5-fold different from donor controls. CA2 was significantly upregulated (1.67-fold) in patients with PAH ($q = 0.000367$). (*E*) CA2 upregulation in IPAH patient lungs was validated by qPCR ($n = 12$ IPAH and $n = 12$ donor lungs). Statistical analysis by Mann-Whitney *U* test. Data represent mean ± SEM (*$P < 0.05$, **$P < 0.01$, and ***$P < 0.001$).

and ACTZ treatment have direct effects on the state of PASMC differentiation in the presence of inflammatory cytokines by restoring a contractile and quiescent phenotype. The antiproliferative effect of ACTZ on PASMCs is in line with previously reported antiproliferative properties of ACTZ in cancer cells (39). Mechanistically, it is important to consider that CA2 is a cofactor for NHE1 (sodium-hydrogen antiporter 1) (40), and inhibition of CA2 has been shown to reduce NHE1 activity (41). NHE1 secretes protons from the cytoplasm and is the main driver of cellular alkalization, which promotes PASMC proliferation in hypoxic PH (42, 43). An increased proton gradient during extracellular acidosis could inhibit NHE1 activity, and CAIs might inhibit NHE1 activity by blocking the cofactor CA2. Potentially, acidosis and CAI might therefore converge on NHE1 inhibition in PASMCs *in vivo*.

The levels of pH used in our *in vitro* studies were substantially lower than what was achieved *in vivo* because we aimed to simulate the local tissue pH (6.8–7.0) that was previously reported in human and preclinical studies rather than to simulate the systemic arterial pH *in vivo* (pH range, 7.08–7.35). The range of extracellular pH in our *in vitro* studies is physiologically relevant and supported by previously published studies in renal epithelial cells (44), hepatocytes (45), endothelial cells (46, 47), cardiac myocytes (48), and VSMCs, as well as in studies of isolated blood vessels (49, 50). These studies have employed a pH range of 6.4–7.4, with a pH value of 6.8 most commonly required for the observed cellular responses. This is consistent with our findings in primary VSMCs, and it is not surprising, given that intracellular pH in VSMCs was reported to be approximately 7.0–7.2 (51). Similarly, recent studies in immune cells (tumor-associated macrophages) employed pH values of 6.6 for *in vitro* studies (22). The findings of these prior studies are consistent with our findings in BMDMs, in which there is a graded response to extracellular acidosis.

Perivascular inflammation is found in different forms of PAH (6), and vascular lesions show diverse leukocyte subsets (4, 6). Because both pan-CAI and systemic metabolic acidosis are not targeted therapies and potential targets such as CA2 are ubiquitously expressed, it is likely that other cell types are affected by our interventions. For example, the reported immunomodulatory effects of CAIs on mast cells (20) might account for some of the antiinflammatory properties of ACTZ in our study. Also, T-cell activation that is known to contribute to PH pathogenesis (3, 52) was shown to be suppressed by metabolic acidosis, and this may contribute to the observed antiinflammatory effects (22).

We acknowledge that ACTZ has other beneficial properties in PAH. It is beneficial in the context of hypoxia, especially at high altitude (53) and in individuals with sleep-disordered breathing (54), and its acute and chronic effects are currently tested in patients with PAH in a clinical trial in Europe (AcuteAZA [Acute Hemodynamic Effect of Acetazolamide in Pulmonary Hypertension]; www.clinicaltrials.gov identifier NCT02755259). In the hypoxic model of PH, ACTZ was shown to mediate some of its protective effects through changes in blood rheology (26), prevention of hypoxic vasoconstriction (55), or changes in ventilation patterns (56). Also, CAIs were implicated in improved nitric oxide bioavailability (57), which might contribute to amelioration of PH. In addition, other CA isoforms, such as CAIX, which is a recognized transcriptional target of hypoxia-inducible factor 1α signaling and is highly upregulated in the endothelium in hypoxic PH (58), might also be affected by CAI treatment.

Current PAH therapies have no appreciable effect on perivascular inflammation, as shown by Stacher and colleagues (6). Also, cytokines implicated in PAH pathogenesis are released from different cell types, and there is redundant activation and interaction of pathways. It is thus unlikely that targeting one specific pathway will be sufficient to result in clinical efficacy (8). Rather, global immune modulation may be a more promising therapeutic strategy. Because ACTZ and other CAIs are currently clinically used drugs with known dose and safety profiles, we propose carbonic anhydrase inhibition as a novel strategy to curb inflammation and restore vascular homeostasis in PAH.

In conclusion, we demonstrate that use of the CAI ACTZ ameliorates severe experimental PH. We propose that ACTZ modulates AM activation via a dual mechanism of macrophage carbonic anhydrase inhibition and systemic metabolic acidosis and restores vascular homeostasis. Collectively, our studies identify a previously unrecognized role of CAs in macrophage activation and provide insight into the therapeutic potential of targeting CA to treat PH and macrophage-mediated inflammation. ■

Author disclosures are available with the text of this article at www.atsjournals.org.

Acknowledgment: The authors acknowledge Maad Alzayer, Fotios Spyropoulos, and April Kwong for technical assistance. Tissue samples and microarray data were provided by the Pulmonary Hypertension Breakthrough Initiative. Bioanalyzer analysis was performed in the Boston Children's Hospital Intellectual and Developmental Disabilities Research Center Molecular Genetics Core Facility.

References

1. Farber HW, Loscalzo J. Pulmonary arterial hypertension. *N Engl J Med* 2004;351:1655–1665.
2. Pugliese SC, Poth JM, Fini MA, Olschewski A, El Kasmi KC, Stenmark KR. The role of inflammation in hypoxic pulmonary hypertension: from cellular mechanisms to clinical phenotypes. *Am J Physiol Lung Cell Mol Physiol* 2015;308:L229–L252.
3. Rabinovitch M, Guignabert C, Humbert M, Nicolls MR. Inflammation and immunity in the pathogenesis of pulmonary arterial hypertension. *Circ Res* 2014;115:165–175.
4. Savai R, Pullamsetti SS, Kolbe J, Bieniek E, Voswinckel R, Fink L, *et al*. Immune and inflammatory cell involvement in the pathology of idiopathic pulmonary arterial hypertension. *Am J Respir Crit Care Med* 2012;186:897–908.
5. Soon E, Holmes AM, Treacy CM, Doughty NJ, Southgate L, Machado RD, *et al*. Elevated levels of inflammatory cytokines predict survival in idiopathic and familial pulmonary arterial hypertension. *Circulation* 2010;122:920–927.
6. Stacher E, Graham BB, Hunt JM, Gandjeva A, Groshong SD, McLaughlin VV, *et al*. Modern age pathology of pulmonary arterial hypertension. *Am J Respir Crit Care Med* 2012;186: 261–272.
7. Steiner MK, Syrkina OL, Kolliputi N, Mark EJ, Hales CA, Waxman AB. Interleukin-6 overexpression induces pulmonary hypertension. *Circ Res* 2009;104:236–244.
8. Groth A, Vrugt B, Brock M, Speich R, Ulrich S, Huber LC. Inflammatory cytokines in pulmonary hypertension. *Respir Res* 2014;15:47.
9. Vergadi E, Chang MS, Lee C, Liang OD, Liu X, Fernandez-Gonzalez A, *et al*. Early macrophage recruitment and alternative activation are critical for the later development of hypoxia-induced pulmonary hypertension. *Circulation* 2011;123: 1986–1995.
10. Minamino T, Christou H, Hsieh CM, Liu Y, Dhawan V, Abraham NG, *et al*. Targeted expression of heme oxygenase-1 prevents the pulmonary inflammatory and vascular responses to hypoxia. *Proc Natl Acad Sci USA* 2001;98:8798–8803.
11. Hashimoto-Kataoka T, Hosen N, Sonobe T, Arita Y, Yasui T, Masaki T, *et al*. Interleukin-6/interleukin-21 signaling axis is critical in the pathogenesis of pulmonary arterial hypertension. *Proc Natl Acad Sci USA* 2015;112:E2677–E2686.
12. Hurst LA, Dunmore BJ, Long L, Crosby A, Al-Lamki R, Deighton J, *et al*. TNFα drives pulmonary arterial hypertension by suppressing the BMP type-II receptor and altering NOTCH signalling. *Nat Commun* 2017;8:14079.
13. Tian W, Jiang X, Tamosiuniene R, Sung YK, Qian J, Dhillon G, *et al*. Blocking macrophage leukotriene B_4 prevents endothelial injury and reverses pulmonary hypertension. *Sci Transl Med* 2013;5: 200ra117.
14. Nicolls MR, Voelkel NF. The roles of immunity in the prevention and evolution of pulmonary arterial hypertension. *Am J Respir Crit Care Med* 2017;195:1292–1299.
15. Frid MG, Brunetti JA, Burke DL, Carpenter TC, Davie NJ, Reeves JT, *et al*. Hypoxia-induced pulmonary vascular remodeling requires recruitment of circulating mesenchymal precursors of a monocyte/macrophage lineage. *Am J Pathol* 2006;168:659–669.
16. Ackers-Johnson M, Talasila A, Sage AP, Long X, Bot I, Morrell NW, *et al*. Myocardin regulates vascular smooth muscle cell inflammatory activation and disease. *Arterioscler Thromb Vasc Biol* 2015;35: 817–828.
17. Tang RH, Zheng XL, Callis TE, Stansfield WE, He J, Baldwin AS, *et al*. Myocardin inhibits cellular proliferation by inhibiting NF-κB(p65)-dependent cell cycle progression. *Proc Natl Acad Sci USA* 2008;105: 3362–3367.
18. Savai R, Al-Tamari HM, Sedding D, Kojonazarov B, Muecke C, Teske R, *et al*. Pro-proliferative and inflammatory signaling converge on FoxO1 transcription factor in pulmonary hypertension. *Nat Med* 2014;20:1289–1300.
19. Christou H, Reslan OM, Mam V, Tanbe AF, Vitali SH, Touma M, *et al*. Improved pulmonary vascular reactivity and decreased hypertrophic remodeling during nonhypercapnic acidosis in experimental pulmonary hypertension. *Am J Physiol Lung Cell Mol Physiol* 2012; 302:L875–L890.
20. Henry EK, Sy CB, Inclan-Rico JM, Espinosa V, Ghanny SS, Dwyer DF, *et al*. Carbonic anhydrase enzymes regulate mast cell-mediated inflammation. *J Exp Med* 2016;213:1663–1673.
21. Youm YH, Nguyen KY, Grant RW, Goldberg EL, Bodogai M, Kim D, *et al*. The ketone metabolite β-hydroxybutyrate blocks NLRP3 inflammasome-mediated inflammatory disease. *Nat Med* 2015;21: 263–269.
22. Pilon-Thomas S, Kodumudi KN, El-Kenawi AE, Russell S, Weber AM, Luddy K, *et al*. Neutralization of tumor acidity improves antitumor responses to immunotherapy. *Cancer Res* 2016;76:1381–1390.

23. Colegio OR, Chu NQ, Szabo AL, Chu T, Rhebergen AM, Jairam V, *et al*. Functional polarization of tumour-associated macrophages by tumour-derived lactic acid. *Nature* 2014;513:559–563.
24. Mogi C, Tobo M, Tomura H, Murata N, He XD, Sato K, *et al*. Involvement of proton-sensing TDAG8 in extracellular acidification-induced inhibition of proinflammatory cytokine production in peritoneal macrophages. *J Immunol* 2009;182: 3243–3251.
25. Supuran CT. Carbonic anhydrases: novel therapeutic applications for inhibitors and activators. *Nat Rev Drug Discov* 2008;7:168–181.
26. Pichon A, Connes P, Quidu P, Marchant D, Brunet J, Levy BI, *et al*. Acetazolamide and chronic hypoxia: effects on haemorheology and pulmonary haemodynamics. *Eur Respir J* 2012; 40:1401–1409.
27. Abe K, Toba M, Alzoubi A, Ito M, Fagan KA, Cool CD, *et al*. Formation of plexiform lesions in experimental severe pulmonary arterial hypertension. *Circulation* 2010;121:2747–2754.
28. Storey JD. The positive false discovery rate: a Bayesian interpretation and the *q*-value. *Ann Stat* 2003;31:2013–2035.
29. Otsuki S, Sawada H, Yodoya N, Shinohara T, Kato T, Ohashi H, *et al*. Potential contribution of phenotypically modulated smooth muscle cells and related inflammation in the development of experimental obstructive pulmonary vasculopathy in rats. *PLoS One* 2015;10: e0118655.
30. El Kasmi KC, Pugliese SC, Riddle SR, Poth JM, Anderson AL, Frid MG, *et al*. Adventitial fibroblasts induce a distinct proinflammatory/ profibrotic macrophage phenotype in pulmonary hypertension. *J Immunol* 2014;193:597–609.
31. Gonzalez NC, Allen J, Blanco VG, Schmidt EJ, van Rooijen N, Wood JG. Alveolar macrophages are necessary for the systemic inflammation of acute alveolar hypoxia. *J Appl Physiol (1985)* 2007; 103:1386–1394.
32. Wen T, Mingler MK, Wahl B, Khorki ME, Pabst O, Zimmermann N, *et al*. Carbonic anhydrase IV is expressed on IL-5-activated murine eosinophils. *J Immunol* 2014;192:5481–5489.
33. El Kasmi KC, Stenmark KR. Contribution of metabolic reprogramming to macrophage plasticity and function. *Semin Immunol* 2015;27: 267–275.
34. Li X, Zhang X, Leathers R, Makino A, Huang C, Parsa P, *et al*. Notch3 signaling promotes the development of pulmonary arterial hypertension. *Nat Med* 2009;15:1289–1297.
35. Xiao Y, Christou H, Liu L, Visner G, Mitsialis SA, Kourembanas S, *et al*. Endothelial indoleamine 2,3-dioxygenase protects against development of pulmonary hypertension. *Am J Respir Crit Care Med* 2013;188:482–491.
36. Ali MS, Starke RM, Jabbour PM, Tjoumakaris SI, Gonzalez LF, Rosenwasser RH, *et al*. TNF-α induces phenotypic modulation in cerebral vascular smooth muscle cells: implications for cerebral aneurysm pathology. *J Cereb Blood Flow Metab* 2013;33: 1564–1573.
37. Li P, Li YL, Li ZY, Wu YN, Zhang CC, A X, *et al*. Cross talk between vascular smooth muscle cells and monocytes through interleukin-1β/interleukin-18 signaling promotes vein graft thickening. *Arterioscler Thromb Vasc Biol* 2014;34:2001–2011.
38. Brenninkmeijer L, Kuehl C, Geldart AM, Arons E, Christou H. Heme oxygenase-1 does not mediate the effects of extracellular acidosis on vascular smooth muscle cell proliferation, migration, and susceptibility to apoptosis. *J Vasc Res* 2011;48:285–296.
39. Mokhtari RB, Kumar S, Islam SS, Yazdanpanah M, Adeli K, Cutz E, *et al*. Combination of carbonic anhydrase inhibitor, acetazolamide, and sulforaphane, reduces the viability and growth of bronchial carcinoid cell lines. *BMC Cancer* 2013;13:378.
40. Li X, Alvarez B, Casey JR, Reithmeier RA, Fliegel L. Carbonic anhydrase II binds to and enhances activity of the Na^+/H^+ exchanger. *J Biol Chem* 2002;277:36085–36091.
41. Vargas LA, Díaz RG, Swenson ER, Pérez NG, Álvarez BV. Inhibition of carbonic anhydrase prevents the Na^+/H^+ exchanger 1-dependent slow force response to rat myocardial stretch. *Am J Physiol Heart Circ Physiol* 2013;305:H228–H237.
42. Huetsch JC, Jiang H, Larrain C, Shimoda LA. The Na^+/H^+ exchanger contributes to increased smooth muscle proliferation and migration in a rat model of pulmonary arterial hypertension. *Physiol Rep* 2016; 4:e12729.
43. Yu L, Quinn DA, Garg HG, Hales CA. Deficiency of the *NHE1* gene prevents hypoxia-induced pulmonary hypertension and vascular remodeling. *Am J Respir Crit Care Med* 2008;177:1276–1284.
44. Feifel E, Obexer P, Andratsch M, Euler S, Taylor L, Tang A, *et al*. p38 MAPK mediates acid-induced transcription of PEPCK in LLC-PK_1-$FBPase^+$ cells. *Am J Physiol Renal Physiol* 2002;283:F678–F688.
45. Haas MJ, Reinacher D, Li JP, Wong NC, Mooradian AD. Regulation of *apoA1* gene expression with acidosis: requirement for a transcriptional repressor. *J Mol Endocrinol* 2001;27:43–57.
46. Terminella C, Tollefson K, Kroczynski J, Pelli J, Cutaia M. Inhibition of apoptosis in pulmonary endothelial cells by altered pH, mitochondrial function, and ATP supply. *Am J Physiol Lung Cell Mol Physiol* 2002;283:L1291–L1302.
47. Agulló L, Garcia-Dorado D, Escalona N, Inserte J, Ruiz-Meana M, Barrabés JA, *et al*. Hypoxia and acidosis impair cGMP synthesis in microvascular coronary endothelial cells. *Am J Physiol Heart Circ Physiol* 2002;283:H917–H925.
48. Vittone L, Mundiña-Weilenmann C, Said M, Mattiazzi A. Mechanisms involved in the acidosis enhancement of the isoproterenol-induced phosphorylation of phospholamban in the intact heart. *J Biol Chem* 1998;273:9804–9811.
49. Ishizaka H, Kuo L. Acidosis-induced coronary arteriolar dilation is mediated by ATP-sensitive potassium channels in vascular smooth muscle. *Circ Res* 1996;78:50–57.
50. Berger MG, Vandier C, Bonnet P, Jackson WF, Rusch NJ. Intracellular acidosis differentially regulates K_V channels in coronary and pulmonary vascular muscle. *Am J Physiol* 1998;275:H1351–H1359.
51. Austin C, Wray S. Interactions between Ca^{2+} and H^+ and functional consequences in vascular smooth muscle. *Circ Res* 2000;86: 355–363.
52. Tamosiuniene R, Tian W, Dhillon G, Wang L, Sung YK, Gera L, *et al*. Regulatory T cells limit vascular endothelial injury and prevent pulmonary hypertension. *Circ Res* 2011;109:867–879.
53. Nieto Estrada VH, Molano Franco D, Medina RD, Gonzalez Garay AG, Martí-Carvajal AJ, Arevalo-Rodriguez I. Interventions for preventing high altitude illness: part 1. Commonly-used classes of drugs. *Cochrane Database Syst Rev* 2017;6:CD009761.
54. Latshang TD, Kaufmann B, Nussbaumer-Ochsner Y, Ulrich S, Furian M, Kohler M, *et al*. Patients with obstructive sleep apnea have cardiac repolarization disturbances when travelling to altitude: randomized, placebo-controlled trial of acetazolamide. *Sleep (Basel)* 2016;39: 1631–1637.
55. Shimoda LA, Luke T, Sylvester JT, Shih HW, Jain A, Swenson ER. Inhibition of hypoxia-induced calcium responses in pulmonary arterial smooth muscle by acetazolamide is independent of carbonic anhydrase inhibition. *Am J Physiol Lung Cell Mol Physiol* 2007;292: L1002–L1012.
56. Swenson ER. Carbonic anhydrase inhibitors and ventilation: a complex interplay of stimulation and suppression. *Eur Respir J* 1998;12: 1242–1247.
57. Aamand R, Dalsgaard T, Jensen FB, Simonsen U, Roepstorff A, Fago A. Generation of nitric oxide from nitrite by carbonic anhydrase: a possible link between metabolic activity and vasodilation. *Am J Physiol Heart Circ Physiol* 2009;297:H2068–H2074.
58. Zhao L, Oliver E, Maratou K, Atanur SS, Dubois OD, Cotroneo E, *et al*. The zinc transporter ZIP12 regulates the pulmonary vascular response to chronic hypoxia. *Nature* 2015;524:356–360.